Effect of Extreme Compression on Diesel Spray Penetration and Dispersion

M. N. Svrcek*, S.L. Miller, and C. F. Edwards
Department of Mechanical Engineering
Stanford University
Stanford, CA 94306 USA

Abstract

Increasing the compression ratio of a simple-cycle engine beyond 100:1 can enable first-law efficiency approaching 60%, if losses relative to the ideal cycle can be maintained similar to existing engines. Achieving this in practice will require understanding and managing the combustion process in the very high gas density that results from such a compression ratio. In addition, a desire to reduce the time scale for heat transfer by more rapid compression and expansion constrains the time available to initiate and complete combustion. The highest ambient density studied in existing combustion-bomb research is around 60 kg/m^3, or approximately equivalent to top dead center for a compression ratio of 53:1. As a first step in characterizing combustion at compression ratios up to 100:1, this paper studies the penetration and dispersion of a vaporizing, non-reacting diesel spray in a free-piston extreme compression device for compression ratios from 30 to 100:1. High-speed schlieren photography through full-bore optical access in the end wall of the combustor provides imaging of the spray. Spray penetration and dispersion via spray angle are measured as functions of time for each compression ratio. The recorded data are compared to the existing literature by use of a correlation developed from the high-ambient-density, combustion-bomb research mentioned above. The data for spray angle correlate reasonably well with expectations extrapolated from the existing literature for all compression ratios studied. Penetration in the extreme compression device was found to correlate very well with the prior research at lower compression ratios, with penetration decreasing as compression ratio is increased. Above 60:1, however, penetration rate did not further decrease as expected, but rather remained essentially constant from 60 to 100:1. This result is explained by the fact that, for the free-piston combustor, the volume profile becomes steeper in time with increasing compression ratio, resulting in the density at start of injection remaining nearly the same as compression ratio is increased from 60 to 100:1. Comparing penetration rate for early and late portions of the injection to correlations for density at that point in time, indicates that the existing correlation continues to predict penetration rate as a function of density even up to densities of 100 kg/m^3.

Introduction

Previous work in our research group set out to understand, based on exergetic considerations, how one should go about improving the thermodynamic efficiency of simple-cycle engines. An important and general result of this work was to demonstrate that in all cases the most effective method of the improving efficiency of a simple-cycle engine is to perform combustion at the highest internal energy state possible, and in particular for a piston engine, to achieve this high energy state via compression work [1]. Operating a piston engine at a compression ratio (CR) of 100:1, for example, could achieve a thermal efficiency approaching 60%, if losses relative to the ideal cycle can be maintained similar to those in existing, lower compression engines.

Successful operation of an engine at 100:1 CR requires solution of several design challenges: handling increased heat transfer due to higher gas temperature, piston sealing to reduce unwanted mass loss, material stress, and control of the combustion process. Handling material stress, in addition to reducing heat transfer by using a more rapid compression and expansion, lead to the use of a free-piston design. The steeper volume profile of the free-piston engine, combined with a desire to reduce the time scale for heat transfer, constrains the time available to initiate and complete combustion. Furthermore, at 100:1 CR the ambient density of the gas is very high, about 1/8 of the fuel density. In order to succesfully manage combustion, we must better understand the behavior of the diesel spray in this high-density environment.

A significant body of research exists on diesel spray penetration and dispersion, but none of which we are aware approach the ambient density experienced in the extreme compression device. In a widely cited study, Hiroyasu et.

*Corresponding author, msvrcek@stanford.edu

al. [2] discuss results for penetration and dispersion up to densities of 30 kg/m^3, but with injection pressures lower than 40 MPa. Another study by Varde and Popa [3] went as high as 40 kg/m^3, along with an injection pressure of 150 MPa. The study that has most closely approached our conditions is the work done in the combustion bomb at Sandia National Laboratory. In particular, Naber and Siebers [4] discuss the effect of density on spray penetration and dispersion up to a density of 60 kg/m^3, roughly equivalent to conditions at TDC for a 53:1 CR. This paper will largely follow the methodology from that study in order to provide a comparison for our own data up to 50:1. The work presented in this paper is a first step towards better understanding the combustion process at extreme compression ratios by investigating the penetration rate and spray angle of vaporizing, non-reacting diesel sprays in a free-piston combustor up to a compression ratio of 100:1.

Experimental Setup and Methodology

We have constructed a free-piston device capable of reaching compression ratios in excess of 100:1. The device is single-shot, without work extraction, and serves as a test-bed for performing research towards developing an extreme compression reciprocating engine. A large reservoir is filled with air to provide the driving gas for the piston. A fast-acting poppet valve introduces the driver air into the section above the piston, which is accelerated down the cylinder bore, reaching speeds in excess of 100 m/s. Near the end of its travel the piston passes into a forged combustor section capable of withstanding high pressure, and which contains the fuel injectors. A schematic of the lower portion of the cylinder and the combustor section is shown in Figure 1. The cylinder bore diameter is 54.1 mm. In order to minimize heat transfer losses, a large volume-to-surface area ratio is desired at the minimum volume (TDC). At 100:1 CR the piston is approximately 25 mm from the end wall, resulting in a cylinder stroke of 2.5 meters.

Conventional piston rings would not survive the speed and pressure obtained here, hence the piston uses graphite rings that act primarily as clearance control, minimizing the gap available for blowby rather than effecting an active seal. Measurement of volume vs. time is achieved by a combination of magnetic reluctance sensors spaced along the length of the cylinder and an optical sensor consisting of a laser diode and photodiode passed through optical fibers in the wall of the cylinder. The optical sensor provides more precise sensing near TDC. Pressure is measured by a piezo-electric transducer mounted in the combustor section. Together these measurements provide the indicated work output of the device. During normal combustion operation the device is run with air in the cylinder. For this study the cylinder was purged prior to each run and filled with pure nitrogen to provide an inert environment in which to study non-reacting sprays, while at the same time maintaining compression characteristics similar to air.

The fuel injection system consists of a Bosch common rail pump, accumulator, and high-pressure diesel injector from a passenger car application. A custom injector nozzle has a single orifice directing the spray across the diagonal of the combustor bore. For all data presented here the orifice diameter was 0.15 mm, and the fuel injection pressure was 150 MPa. A sapphire window mounted in the bottom of the combustor provides full-bore optical access to the cylinder. A schlieren system was constructed for visualizing the spray, and is shown schematically along with the combustor in Fig. 1. Laser light at 488 nm is collimated through a large achromatic lens and passed into the cylinder. It reflects off a mirror bonded to

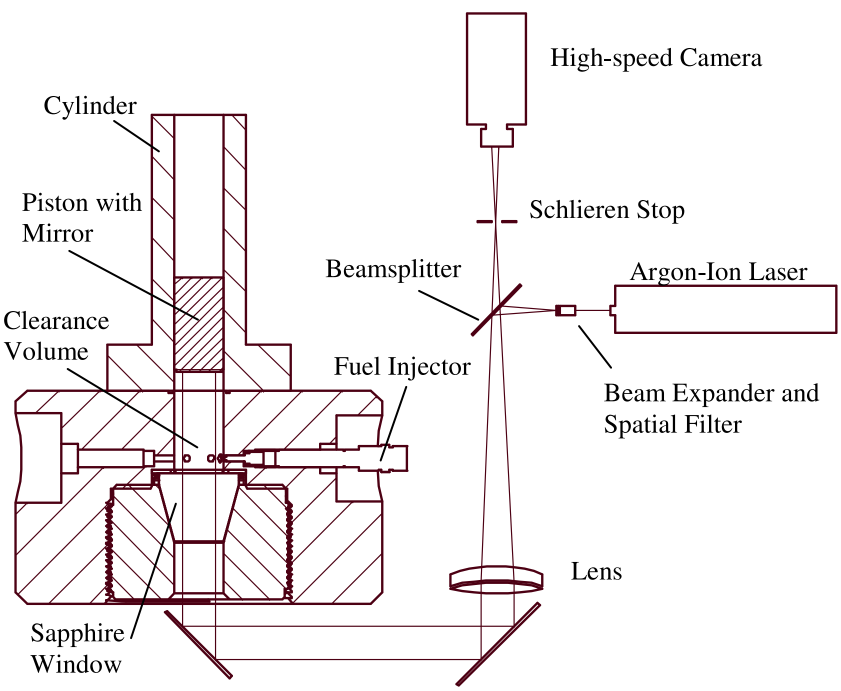

Figure 1. Schematic of experimental setup.

the face of the piston, and returns through the same achromat to a high-speed digital camera. A beamsplitter allows the incoming and outgoing beams to lie on the same axis. The injector plane is located at one focal point of the achromat with the camera lens focused near infinity, while a schlieren stop is placed at the other focal point and can be adjusted to change the schlieren sensitivity.

Figure 2 shows a sample image along with the resulting binary image defining the spray region. For this study the camera operated at a framing rate of 36,000 frames per second, with an exposure of 10 μs and a resolution of 256 x 256 pixels. Schlieren sensitivity was chosen to optimize the visibility of the spray relative to the background gas, however a large degree of small-scale turbulence is still visible in the background. This is likely due to fluid turbulence generated by the piston during the compression stroke, interacting with the boundary layers on the window surface and piston mirror surface. In addition, in this setup the schlieren beam passes through the test section twice, increasing the sensitivity.

The spray region within the image is defined by the following four steps. First, the image is converted to grayscale and a median filter applied to it to reduce the small-scale background while maintaining the spray edge. Second, a reference image taken immediately prior to the spray is subtracted from the spray image. Due to the amount of dynamic background, the reference image is heavily filtered so that only the static, largest-scale variations in intensity are canceled when subtracted, for example the darkening near the wall of the cylinder. Third, regions of the image below an intensity cutoff are identified, one of which is the spray. A number of small areas of the background turbulence may also be below the threshold; the spray is defined by finding the contiguous region attached to the location of the fuel injector tip. The methods used to measure penetration and angle inherently average out small areas of dark background that might coincide with the spray boundary. Fourth, the spray axis is defined as passing through the injector tip and the centroid of the spray region , as shown by the dashed line in Fig. 2.

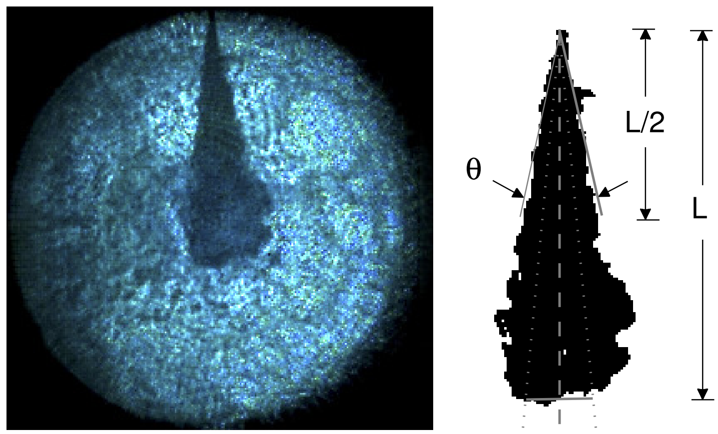

Figure 2. Image from camera and resulting processed spray, showing penetration length and spray angle. Image is from 90:1 compression ratio, 0.6 ms after start of injection.

Following the work of Naber and Siebers [4], dispersion of the spray is quantified with a single spray angle corresponding to the angle of a triangle whose area is equal to the projected area of the upstream half of the spray. The half spray angle ($\theta / 2$) is thus:

$$\frac{\theta}{2} = \tan^{-1}\left(\frac{A_{p,L/2}}{(L/2)^2}\right) \qquad (1)$$

where $A_{p,L/2}$ is the projected area and L the spray penetration. Using only the upstream half of the spray to define dispersion reduces variability due to the unsteady head of the spray. A local spray angle at various axial locations along the spray can also be found, but is omitted in this set of results due to space constraints. The spray penetration is then defined as the location in the spray where half of the pixels in the arc subtending $\theta/2$ are dark. Since the spray angle and penetration are interdependent, they are computed iteratively. Finally, knowing that the diameter of the visible portion of the cylinder (that which is spanned by the piston mirror) is 50.8 millimeters, the conversion from pixels to spray geometry in millimeters is obtained.

Results and Discussion

Results were obtained for compression ratios of 30, 45, 60, 70, 80, 90, and 100:1. Figure 3 shows the penetration data as a function of time. For each of the 30:1 and 45:1 cases, two experiments are shown to illustrate the repeatability. The maximum variation from one experiment to the next was approximately 2 mm, or 5% of the full penetration. Similar repeatability was found at the higher compression ratios. The lines are calculated from a correlation developed by Naber and Siebers [4]. The correlation takes a non-vaporizing spray correlation from Wakuri, et. al. [5] and non-dimensionalizes using characteristic time and length scales. The resulting correlation showed good agreement with their vaporizing spray data, in particular for the highest densities they considered. The correlation is a function of nozzle geometry, such that using this correlation allows comparsion to our data while accounting for our smaller nozzle orifice. For all correlations shown in this study, the fuel density is 843 kg/m^3, fuel pressure is 150 MPa, and the nozzle orifice is 0.15 mm with a discharge coefficient of 0.6 and a contraction coefficient of 0.9. The correlation is also a function of the gas density and pressure. Two points must be considered when using the correlation for the compression device. First, piston sealing is not perfect in the device, resulting in gas density that is somewhat less than that calculated directly from the compression ratio. Hence, for all of the correlations and density plots shown in this study, density is calculated from the experimental pressure measurements, assuming isentropic compression of the gas core. Second, during the course of injection the gas density and pressure continue to change as the piston advances. In the correlations shown in Fig. 3, the time-averaged conditions during injection for each compression ratio are used. For this study, injection started 1 ms before TDC and ended at TDC, which is a reasonable approximation of actual engine operating conditions.

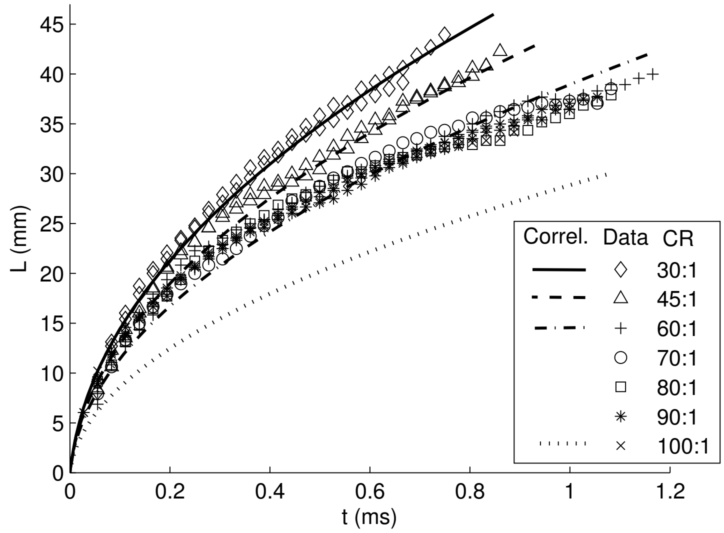

Figure 3. Penetration vs. time. Correlations from Naber and Siebers [4], using average conditions during injection.

For the 30:1 and 45:1 cases, the measured penetration data are in agreement with the corresponding correlations, indicating good agreement with the results found in [4]. Above 60:1, however, the spray penetration rate does not decrease further with increasing compression ratio. As shown in Fig. 3, the penetration profiles for 60:1 up to 100:1 lie essentially on top of one another. The lowest solid line plotted in Fig. 3 is the correlation for average conditions during injection at 100:1, indicating that one would expect spray penetration to continue to decline as compression ratio increases. The work done by Naber and Siebers [4] demonstrated that ambient gas density is one of the primary factors affecting spray penetration, and a closer examination of the time-variation of density during injection, particularly for the free piston, can provide an understanding of the behavior seen above 60:1.

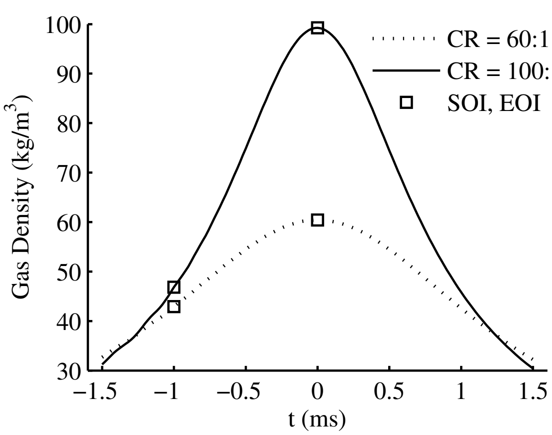

Figure 4. Gas density vs. time for two compression ratios. SOI, EOI are start and end of injection

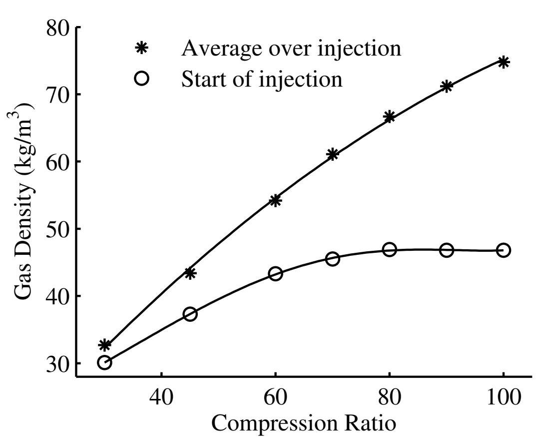

Figure 5. Gas density vs. compression ratio at the start of injection and averaged over the course of injection.

Figure 4 shows experimental traces of density versus time for a 60:1 and 100:1 compression ratio, with start and end of injection marked. Because the free-piston dynamics are dictated by the pressure force balance on the piston, at higher compression ratios the volume profiles are steeper in time. In Fig. 4 one can see that for the 60:1 case the density at start of injection is about 30% less than at end of injection, but for 100:1 the density at SOI is reduced by nearly 60%. This trend can be seen more clearly in Fig. 5, which shows that while gas density averaged over the course of injection continues to rise nearly linearly, the density at start of injection becomes nearly constant above 60:1. In addition, Fig. 6 shows penetration vs. time for the 90:1 and 100:1 CR runs, along with two correlations: one for gas density corresponding to the start of injection, and one corresponding to the density at end of injection. Two conclusions can be drawn from these combined results. First, the fact that the penetration vs. time profiles for 60:1 through 100:1 collapse onto one another, combined with the roll-off in density at start of injection seen above 60:1 in Fig. 5, indicates that the ambient conditions during the early part of the spray dominate the overall penetration profile. This result is consistent with the $t^{1/2}$ dependence of the penetration shown by Hiroyasu and Arai [2] and apparent in the penetration profiles shown in this paper. Second, the penetration data in Fig. 6 closely follow the correlation for conditions at start of injection for the early part of the spray, and closely match the slope of the correlation for conditions at the end of injection during the latter part of the spray. The matching slopes near the end of injection suggest that the penetration rate as a function of density continues to be well predicted by the correlation, even for densities far higher than those for which the correlation was developed.

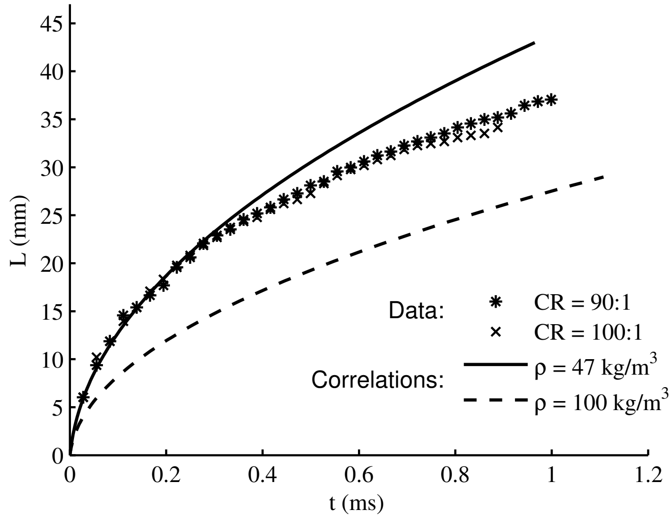

Figure 6. Penetration vs. time data for 90 and 100:1. Correlations from Naber and Siebers [4], for gas density found at start and end of injection for CR = 100:1.

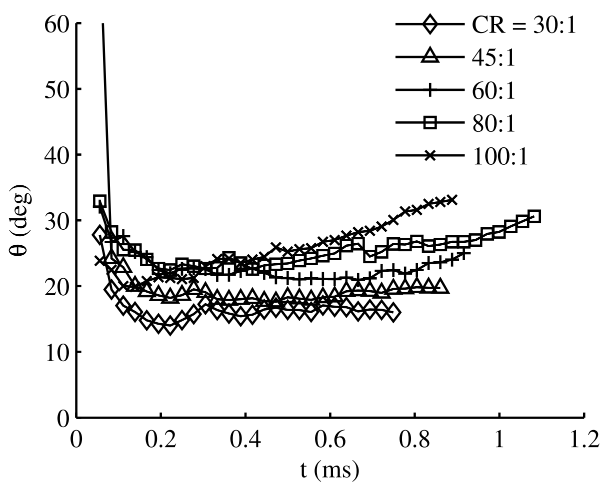

Figure 7. Spray angle vs. time.

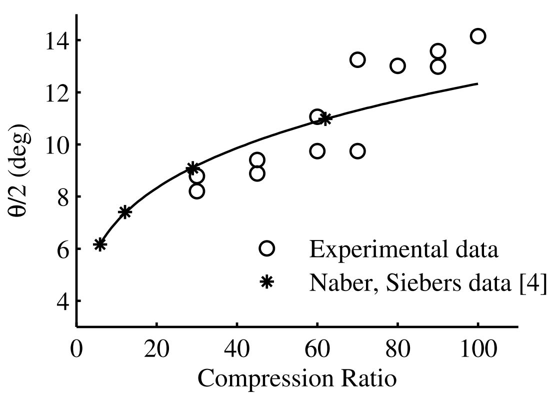

Figure 8. Average spray angle during quasi-steady spray, vs. compression ratio.

Spray angle as defined in the previous section was also calculated versus time for each experiment; several of these are plotted in Fig. 7. Repeatability between experiments was slightly worse for spray angle than for penetration, with angle variation around 15%. This is most likely due to the turbulent nature of the boundary of the spray, combined with the small-scale background turbulence in the schlieren image coinciding with the spray boundary (to which spray angle is more sensitive than penetration). After an initial settling, the spray angle is essentially constant for the duration of the spray event for the lower compression ratios. This 'quasi-steady' portion of the spray has been observed in numerous studies [2- 4]. Naber and Siebers [4] also demonstrated that spray angle increases with increasing ambient gas density. To observe this trend, Fig. 8 shows spray angle averaged over the quasi-steady portion of the spray, as a function of compression ratio. This angle was taken as an average of the points in a given run more than 0.4 ms after start of injection. The asterisks are data points directly from [4] with the ambient density from their experiments converted to average conditions for a given CR. The solid line is a power law fit to the data from [4]. For all compression ratios, the spray angle roughly follows the expected trend, increasing slightly more than expected with increasing compression ratio. In addition, the effect of time-varying density during compression discussed above for penetration appears for spray angle as well; the spray angle vs. time steadily increases later in the injection for the highest compression ratios in Fig. 7.

Conclusion

Engine efficiency approaching 60% can potentially be realized by performing combustion at compression ratios at or above 100:1. In order to succesfully operate at such extreme conditions, the combustion process must be understood and managed. To that end this paper described the results of a spray penetration and dispersion investigation performed in a free-piston combustor up to a compression ratio of 100:1, using optical access and schlieren imaging of the spray. The results were compared to correlations and data from the previous highest-density spray penetration and dispersion study available. Spray dispersion, as measured by spray angle, essentially followed the expected trends from the prior research. Spray penetration also agreed well with the existing literature at the lower compression ratios, however, from 60:1 to 100:1 the spray penetration rate was found to remain virtually constant, contrary to the expected trend of penetration continuing to decrease with increasing compression ratio. This behavior was explained by the density profile of the free-piston combustor becoming more compact in time at high compression ratios—resulting in the density at start of injection remaining roughly constant above 60:1. The collapse of penetration profiles onto one another, corresponding with the roll-off of density at start of injection also above 60:1, indicates that conditions during the early portion of the injection dominate the overall penetration of the spray. Furthermore, comparison of the earlier and later stages of a given penetration profile to separate correlations for density at start and end of injection, indicate that in fact the spray correlation continues to predict the penetration rate well even for gas densities far higher than those for which the correlation was originally developed.

References

1. Teh, K.-Y., Miller, S. L., and Edwards, C. F., *International Journal of Engine Research* 9:449-481 (2008).
2. Hiroyasu, H., and Arai, M., *Transactions of the SAE* 99:1050-1061 (1990).
3. Varde, K., and Popa, M., *Transactions of the SAE* 92:265-278 (1983).
4. Naber, J. D., and Siebers, D. L., "Effects of Gas Density and Vaporization on Penetration and Dispersion of Diesel Sprays," SAE Paper 960034, 1996.
5. Wakuri, Y., Fujii, M., Amitani, T., and Tsuneya, R., "Studies of the Penetration of Fuel Spray in a Diesel Engine," Bulletin of JSME, Vol. 3, No. 9, 1960.